

UDC 621.793:621.891

STRUCTURE-PHASE CONDITION AND TRIBOLOGICAL PROPERTIES OF COATINGS BASED ON SELF-FLUXING NICKEL ALLOY PG-12N-01 AFTER LASER SURFACING

O. G. Devoino,¹ E. É. Feldshtein,² M. A. Kardapolova,¹ and N. I. Lutsko¹

Translated from *Metallovedenie i Termicheskaya Obrabotka Metallov*, No. 12, pp. 51 – 55, December, 2016.

Some parameters of laser surfacing of self-fluxing nickel alloy PG-12N-01 are considered. Different structures containing a low-melting γ -Ni – Ni₃B eutectic and a γ -Ni – Cr₃C₂ eutectic that crystallizes at a higher temperature and forms the strength skeleton of the coating may form depending on the rate of the surfacing. The effect of the rate of the surfacing on the wear resistance of the coating and on the coefficients of dry friction are determined.

Key words: laser surfacing, nickel alloy, structure and phase composition, friction coefficient, wear intensity.

INTRODUCTION

Wear-resistant coatings play an important role in elevation of reliability of machine parts and machines. Such coatings are deposited by various methods including the galvanic technique, cladding, electric spark hardening, surfacing in an electric arc or in a plasma jet and with the help of electron and ion beams, laser radiation, etc.

Laser processes are applied widely due to universality of the equipment and a wide spectrum of technological possibilities [1 – 3]. Reports have appeared on optimization of the process parameters of laser surfacing [4, 5], and formation of coatings with different structures [4, 6 – 8], mechanical, physical and operating properties [9 – 11].

The working surfaces of parts are mainly hardened with the use of three groups of materials, i.e., self-fluxing alloys based on iron, nickel, and cobalt [12 – 14]. The nickel- and cobalt-base alloys possess good wettability, deoxidizing and flux-forming capacities [12], high physical and mechanical characteristics [13, 14] and a high resistance to wear, oxidation and high-temperature corrosion [15, 16].

The aim of the present work was to analyze the effect of the conditions of laser surfacing on the geometry and structural and phase states of a coating based on self-fluxing nickel alloy PG-12N-01.

METHODS OF STUDY

The self-fluxing nickel alloy PG-12N-01 used for the coating had the following chemical composition (in wt.%): 0.3 – 0.6 C, 1.7 – 2.2 B, 1.2 – 3.2 Si, 8 – 14 Cr, 1.2 – 1.3 Fe, the remainder Ni.

The coating was deposited onto a substrate from steel 45 by laser surfacing. The initial powder was sieved to a grain size of 20 – 80 μ m using a set of sieves and then dried in an electric furnace at 200°C for 2 h. The coating was deposited with the help of a “Kometa 2” CO₂ gas continuous laser with a power of 1 kW. The powder was fed into the working zone at a rate of 8 – 20 g/min coaxially to the laser beam through a specially designed nozzle. A schematic diagram of the process is presented in Fig. 1a.

The deposition was conducted in speed range of 40 – 120 mm/min at a distance of 10, 12 and 14 mm with a step of 1.2 mm. The beam diameter was taken to be 1 mm; the power density of the laser radiation was 1.27×10^5 W/cm². The coefficient of overlapping of single tracks after the surfacing was taken to be equal to 0.25.

After the surfacing, the specimens were cut in the direction perpendicular to the beads. We prepared transverse laps of the surfaced zones and then determined the width l and height h of the beads (Fig. 1b). The sizes of individual beads were determined with the help of a “Micro R200” metallographic microscope.

The microstructure of the deposited beads and of the transition zone was studied under a “Mira” scanning electron microscope.

¹ Belarus National Technical University, Minsk, Belarus (e-mail: scvdmmed@bntu.by).

² Zielona Gora University, Zielona Gora, Poland (e-mail: E.Feldshtein@ibem.uz.zgora.pl).

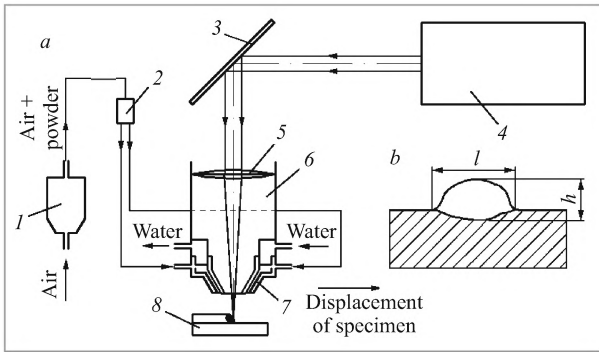


Fig. 1. Scheme of laser surfacing (a) and sizes of the deposited bead (b): 1) powder feeder; 2) distribution of gas-powder mixture; 3) system of rotary mirrors; 4) laser unit; 5) focusing lens; 6) building-up head-objective; 7) surfacing coaxial nozzle; 8) surfaced specimen.

The tribological tests were performed under the conditions of dry friction with the help of a MIPT unit, (a module for investigation of friction processes) entering an AKIPT automated facility for investigation of friction processes [17]. The tests were based on reciprocating motion of a pin over a specimen (a ‘diamond pin – plane’ scheme for the wear tests and a ‘ball – plane’ scheme for the determination of the sliding friction coefficient as the ratio of the friction force to the force of normal pressure). The force of normal pressure acting normally to the surfaces in contact was created by a set of weights. The friction force was detected with the help of strain meters; the friction coefficient was calculated automatically and recorded in the coordinates ‘friction coefficient – friction path.’ The rider in the wear tests had the form of a grip with fastened diamond tip of a Rockwell device. The normal load was 2 N, the speed of motion of the carriage was 5 mm/sec, the length of one pass was 15 m, the friction path was about 10 m. The wear was evaluated as the volume of the worn-off material determined with the help of a ‘‘Profi-130’’ profilograph-profilometer for measuring the depth and width of the wear track. The volume of the worn-off material was calculated by the formula $V = 0.5bhl$, where b is the width of the wear track, h is the depth of the wear track, and l is the length of a single pass. The wear in-

tensity referred to 1 km of the friction path was determined by the formula $I_v = 100V$.

The rider for determining the friction coefficient had the form of a ball 3 mm in diameter from hardened steel ShKh15. The friction conditions were as follows: speed of motion of the carriage 5 mm/sec, length of single pass 15 mm, friction path 10 m, normal load on the indenter 0.2 N. The friction coefficient was calculated as a mean of the set of instantaneous values corresponding to the horizontal region of the curve in the final stage of the test.

RESULTS AND DISCUSSION

The width of the beads increases with decrease in the distance of surfacing (Fig. 2a). In this case the laser beam is defocused somewhat, the heated spot increases and, as a consequence, the width of the bead increases too. The speed of the surfacing also affects the width of the bead, though to less degree.

The height of the beads also depends on the mode of laser surfacing. With growth of the surfacing distance the energy passing to the molten pool decreases, but the height of the bead increases. The effect of the speed of surfacing on the height of the beads is more substantial (Fig. 2b).

The structure of the coating depends on the parameters of laser surfacing and on the position of single beams on the surface of the substrate (see Fig. 3). At low speeds of displacement of the laser beam the structure of the deposited layer has a dendritic pattern with dendrite arms oriented in the direction of heat removal (Fig. 3a and b); individual particles of the nickel-base solid solution acquire a globular shape (Fig. 3c). When the speed of displacement of the laser beam is doubled, the structural components are refined (Fig. 3d and e). By the data of the x-ray diffraction studies [18] a fusible γ -Ni–Ni₃B eutectic and a carbide γ -Ni–Cr₃C₂ eutectic form in the dendrite space (Fig. 3f). The presence of these eutectics is also confirmed by the microscopic x-ray spectrum analysis in the characteristic radiation (see Fig. 4).

The differences in the structures are explainable by the conditions of heat exchange between the layer of the fused coating and the substrate. When the beads are deposited with the aim of reduction of oxide films, additional time is re-

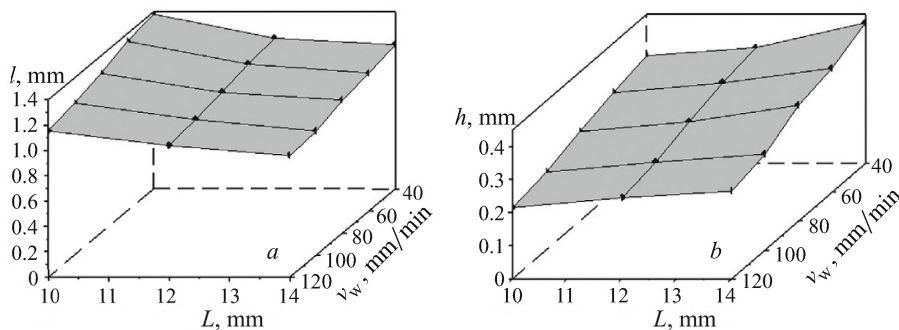


Fig. 2. Dependence of the width l (a) and of the height h (b) of a bead on the speed v_s and distance L of surfacing.

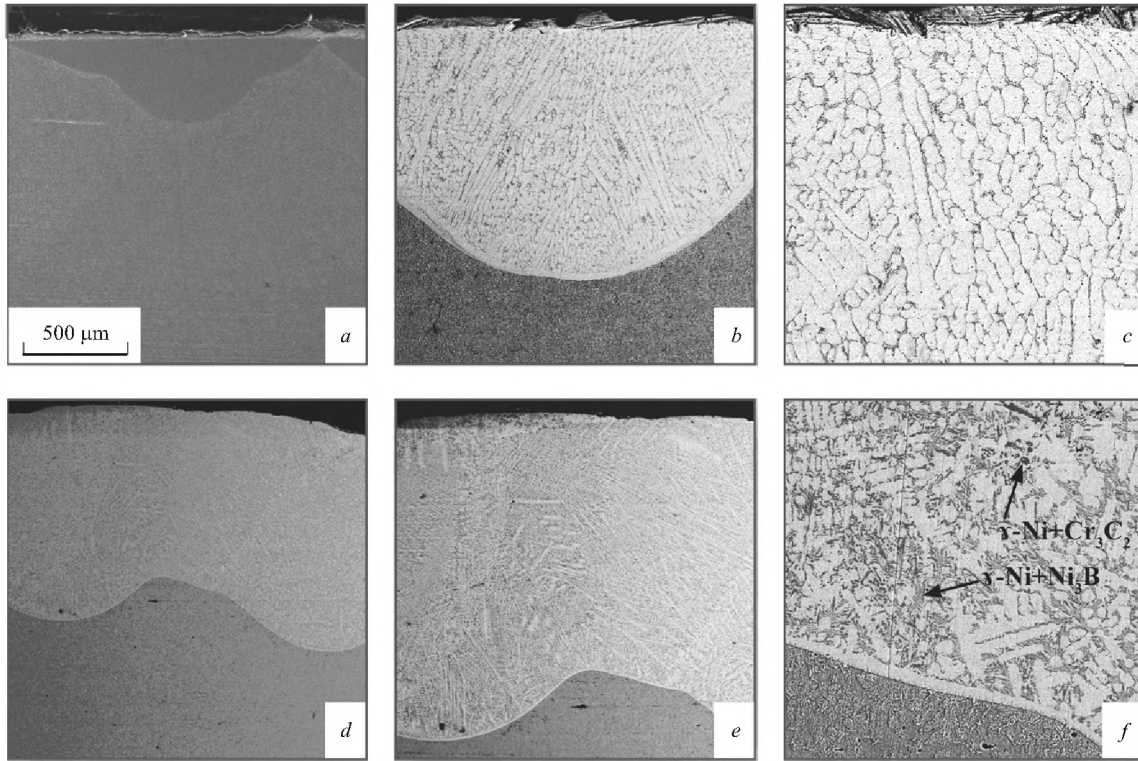


Fig. 3. Microstructure of a coating based on nickel alloy PG-12N-01 deposited onto a substrate of steel 45 by the method of laser surfacing at a speed of the laser beam of 80 mm/min (*a–c*) and 160 mm/min (*d–f*) and a surfacing distance of 12 mm.

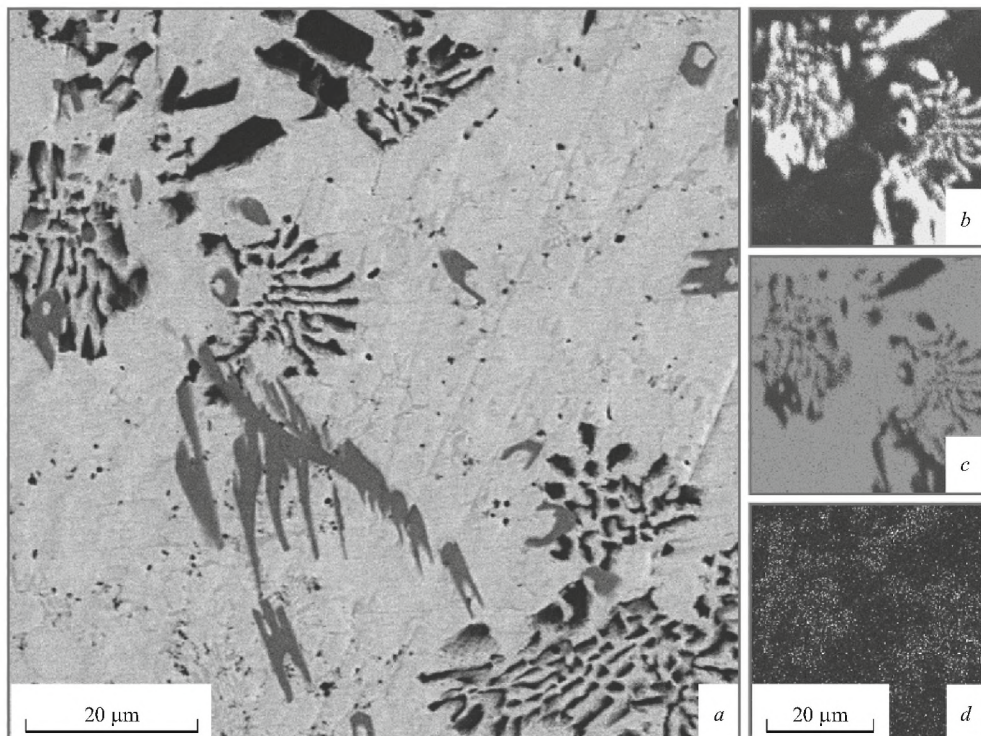


Fig. 4. Electron micrograph (*a*) and results of microscopic x-ray spectrum analysis in Cr (*b*), Ni (*c*), and B (*d*) radiation of regions of a coating based on alloy PG-12N-01 deposited onto a substrate of steel 45 by the method of laser surfacing.

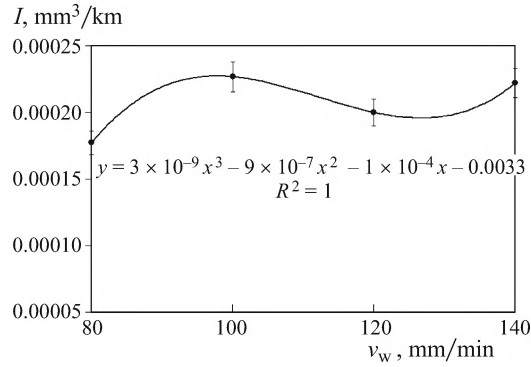


Fig. 5. Effect of the speed of surfacing (v_s) on the intensity of wear (I) of the coating.

quired. It includes the time of reduction of oxide films between the substrate and the surfaced layer, between the powder particles, and between the layers. The regions adjoining the neighbor layer are subjected to a double temperature effect, as a result of which the size of the dendrites near the edge of the bead somewhat increases. The transition zone with a thickness of 40 – 100 μm depending on the surfacing mode, reflects the presence of chemical bonding between the deposited layer and the substrate.

With growth of the speed and of the distance of the surfacing, the structural components are refined and acquire a quasi-eutectic pattern. Since the dendrites crystallize at an angle of 45° to the surface, the most close-packed plane of the crystal lattice [111] is located on the surface.

We have mentioned that the structure is represented by eutectics of two kinds, i.e., $\gamma\text{-Ni} - \text{Ni}_3\text{B}$ with melting temperature 1000°C and $\gamma\text{-Ni} - \text{Cr}_3\text{C}_2$ that crystallizes at higher temperatures and forms the strength skeleton of the coating. Secondary borides crystallize in the form of small nuclei and do not have time to grow, i.e., the strength skeleton of the coating provides a high corrosion resistance in alkalis and acids, and the fusible eutectic cures the pores, cracks and other single defects [18].

The structural and phase condition of the coating layer influences directly its tribological characteristics. With increase of the speed of surfacing the wear resistance of the coating changes (Fig. 5). At low speeds of surfacing and high thermal power passing into the coating, the formed structure is coarse-grained and the distribution of the hardening phases is uniform, which affects the wear resistance favorably. When the speed of the surfacing is increased and the thermal power decreased, the grains become smaller and the bulk wear decreases. With further increase of the treatment speed the fusion of the material of the beads over grain boundaries becomes incomplete, and the bulk wear increases despite the decrease in the grain sizes. It should be noted that the surfacing speeds of about 80 mm/min and about 120 mm/min are the best for the coating studied.

The dependences of the friction coefficient on the friction path are presented in Fig. 6a. For the coatings deposited

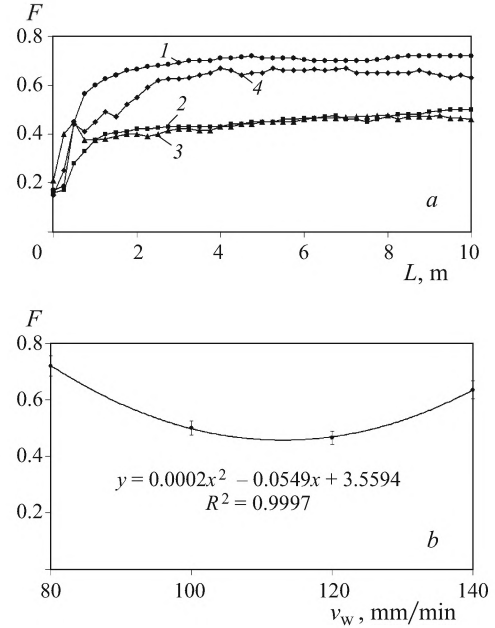


Fig. 6. Friction coefficient (F) as a function of the friction path L (a) and of the speed of surfacing v_s (b): 1) $v_s = 80$ mm/min; 2) $v_s = 100$ mm/min; 3) $v_s = 120$ mm/min; 4) $v_s = 140$ mm/min.

at low speeds (80 and 100 mm/min) the friction coefficient grows rather fast in the initial period (on a friction path of up to 1 m) due to breaking-in of the rubbing surfaces. There is no seizure on these regions, because the friction coefficient does not change abruptly. In the range of 4.5 – 7 m of the friction path the friction coefficient grows slowly. In the last region of the path the friction process stabilizes and the friction coefficient remains virtually unchanged.

For the coatings deposited at high speeds (120 and 140 mm/min) the dependences of the friction coefficient on the friction path are somewhat different. At the beginning of the friction path (up to 0.5 m) the friction coefficient grows rapidly and exhibits jumps indicating seizure. In the range of 6 – 7 m the friction coefficient increases more slowly and seizure of the contacting surfaces still occurs. In the last region of the friction path, just as at lower surfacing speeds, the friction coefficient is rather steady. The processes of seizure in the coatings deposited at a speed of 120 and 140 mm/min are caused by the lower thermal power passing into the coating. This results in incomplete fusion of the material of the beads over grain boundaries and spalling of particles of the coating material, which become nuclei for the seizure process.

Having analyzed the friction coefficients in the final regions of the friction paths (the conditions of stabilization) we may recommend the speeds of surfacing equal to 110 – 120 mm/min for the best friction conditions (Fig. 6b). This dependence of the friction coefficient on the speed of surfacing is explainable by the fact that at $v_s = 80$ mm/min the heat content in the coating is high and promotes formation of a

coarse-grained structure with a low hardness [10], which explains the friction coefficient of about 0.7. When the surfacing speed is increased to 100 – 120 mm/min, conditions are created for formation of an optimum grain structure in the coating and a high enough hardness; the friction coefficient decreases to 0.45 – 0.5. At a higher speed of surfacing and heat content in the coating, the role of incomplete fusion of the material of the beads to grain boundaries becomes important; the hardness increases, and so does the friction coefficient.

CONCLUSIONS

1. Depending on the speed of laser surfacing with self-fluxing nickel alloy PG-12N-01 the structure of the coating may be homogeneous or contain a considerable number of dendrites. The structure of the alloy is represented by eutectics of two kinds, i.e., γ -Ni – Ni₃B with melting temperature 1000°C and γ -Ni – Cr₃C₂ that crystallizes at a higher temperature and constitutes the strength skeleton of the coating.

2. With increase of the speed of surfacing the wear resistance of the coating changes due to structural changes. The best results are obtained at low (about 80 mm/min) speeds of surfacing, which provide a more homogeneous structure, and at high rates of surfacing (about 120 mm/min), which provide refinement of grains. The growth in the wear resistance may attain 30%.

3. The lowest dry friction coefficients are obtained at the speeds of surfacing equal to 110 – 120 mm/min. Depending on the speed of the surfacing, the friction coefficient stabilizes after 0.5 m of the friction path.

REFERENCES

1. C. T. Kwok, *Laser Surface Modification of Alloys for Erosion and Corrosion Resistance*, Woodhead Publ. Ltd, Cambridge (2012).
2. J. C. Ion, *Laser Processing of Engineering Materials. Principles, Procedure and Industrial Application*, Elsevier Ltd, Cambridge (2005).
3. M. J. Dutta and L. Manna, "Laser material processing," *Int. Mater. Rev.*, **56**, 341 – 388 (2011).
4. V. E. Arkhipov, A. A. Ablayev, and L. T. Krasnov, "Structure and properties of coatings deposited by CO₂-laser radiation," *Metalloved. Term. Obrab. Met.*, No. 7, 18 – 21 (1992).
5. V. E. Arkhipov, G. V. Moskvitin, A. N. Polyakov, and N. V. Shirokova, "On the problem of lowering losses in laser surfacing," *Uproch. Teckhnol. Pokr.*, No. 8, 14 – 19 (2010).
6. E. I. Tesker, V. A. Gur'ev, and C. E. Tesker, "Microstructure and properties of laser-surfaced layers," *Fiz. Khim. Obrab. Mater.*, No. 1, 35 – 38 (2004).
7. S. A. Astapchik, A. G. Maklakov, G. G. Goranskii, and V. M. Anisimov, "Laser surfacing of amorphized iron-base powder," *Vestsi Nats. Akad. Navuk Belarusi, Ser. Fiz.-Tekh. Navuk*, No. 2, 5 – 9 (2008).
8. P. N. Koreshkov, V. N. Petrovskii, P. S. Dzhumaev, and V. I. Pol'skii, "Technological features of formation of structure of laser facings with application of radiation of powerful fiber lasers," *Metalloved. Term. Obrab. Met.*, No. 5, 30 – 34 (2014).
9. V. E. Arkhipov, A. A. Alabaev, and L. T. Krasnov, "Physicomechanical characteristics of coatings deposited by laser radiation," *Svaroch. Proizvod.*, No. 1, 18 – 20 (1992).
10. O. G. Devoino, M. A. Kondratova, N. I. Lutsko, and O. N. Koval'chuk, "Formation of single-layer composite banded laser-surfaced coatings from alloy PG-12N-01 and bronze PG-19M-0," in: *Advanced Methods and Processes of Creation and Treatment of Materials, Book 2. Processes and Equipment for Mechanical and Physicotechnical Treatment* [in Russian], MFTI NAN Belarusi, Minsk (2013), pp. 177 – 184.
11. A. G. Grigor'yants, A. I. Misyurov, I. N. Shiganov, et al., "Comparison of corrosion resistances of coatings from cobalt and nickel alloys deposited by laser radiation," *Vestn. MGTU Im. N. É. Baumana, Ser. Mashinost.* (2012), pp. 174 – 180.
12. Y. Ju, S. Y. Guo, and Z. Q. Li, "Status and development of laser surface alloying and laser cladding in China," *Mater. Sci. Eng.*, **20**(1 – 2), 143 – 145 (2002).
13. I. Hemmati, R. M. Huizenga, V. Ocelik, and J. Th. M. De Hosson, "Microstructural design of hardfacing Ni – Cr – B – Si – C alloys," *Acta Mater.*, **61**(16), 6061 – 6070 (2013).
14. Xin Tong, Fu-hai Li, Min Liu et al., "Thermal fatigue resistance of non-smooth cast iron treated by laser cladding with different self-fluxing alloys," *Optics Laser Technol.*, **42**(7), 1154 – 1161 (2010).
15. E. Fernández, M. Cadenas, R. González, et al., "Wear behavior of laser clad NiCrBSi coating," *Wear*, **259**(7 – 12), 870 – 875 (2005).
16. H. Chen, C. Xu, J. Qu, et al., "Sliding wear behavior of laser clad coatings based upon a nickel-based self-fluxing alloy co-deposited with conventional and nanostructured tungsten carbide – cobalt hard metals," *Wear*, **259**(7 – 12), 801 – 806 (2005).
17. <http://belisa.org.by/other/catalog17/projectc885.html?projectSN=20082544-001>.
18. O. G. Devoino, A. S. Kalinichenko, and M. A. Kardapolova, *Modifying Coating Surfaces with the Use of Laser Heating* [in Russian], BNTU, Minsk (2013), 228 p.